The electromagnetic effect of the Mn^{4+} content in $LaMn_{1-x}Ni_xO_3$ ($0 \leq x \leq 0.1$)

2002 J. Phys.: Condens. Matter 14 1075

(http://iopscience.iop.org/0953-8984/14/5/312)

INSTITUTE OF PHYSICS PUBLISHING JOURNAL OF PHYSICS: CONDENSED MATTER

J. Phys.: Condens. Matter **14** (2002) 1075–1083 PII: S0953-8984(02)28169-2

The electromagnetic effect of the Mn^{4+} content in $LaMn_{1-x}Ni_xO_3$ ($0 \leqslant x \leqslant 0.1$)

A Yamamoto and K Oda

Institute of Industrial Science, University of Tokyo, 4-6-1 Komaba, Meguro-Ku, Tokyo 153-8505, Japan

E-mail: akio@iis.u-tokyo.ac.jp

Received 23 August 2001, in final form 23 November 2001
Published 25 January 2002
Online at stacks.iop.org/JPhysCM/14/1075

Abstract

We report on magnetic and electronic properties of ceramic $LaMn_{1-x}Ni_xO_{3+\alpha}$ ($0 \leqslant x \leqslant 0.1$). The purpose of the study is to control the Mn^{4+} concentration by doping Ni into Mn sites and to clarify the influence on the properties of the colossal-magnetoresistance (CMR) effect. All of the samples show the CMR effect. While the $x = 0$ sample exhibits a metal–insulator transition, the others do not. To analyse the dependence of the Curie temperature, T_C, on x, we apply a model concerning polarons associated with electronic localization. And to determine the relation between the Mn^{4+} concentration and the content of Ni ($=x$) doped into Mn sites, we apply Varma's model. We suggest a relation between the Mn^{4+} concentration and x for this series in order to explain the positive dependence of the concentration on x.

1. Introduction

The perovskite manganites $La_{1-x}A_xMnO_3$ (A = Ca, Sr, etc) are known to show a negative CMR effect [1–5]. When the partial replacement of La^{3+} by A^{2+} ions causes the conversion of Mn^{3+} to Mn^{4+}, the magnetic and transport properties of the manganites change. The mixed valency of Mn ions leads to strong ferromagnetic (FM) interaction arising from the Mn^{3+}–O–Mn^{4+} bonds. In general it is considered that this FM interaction originates from the double-exchange (DE) mechanism proposed by Zener [6]. Recently some studies have been made to investigate the effect of the partial replacement not only of A sites but also of B sites, in compounds such as $La_{1-x}A_xMn_{1-y}B_yO_3$ (B = Ni, Co, Fe, etc) [7–11, 20, 21]. According to these studies, as the level of replacement of B sites increases, T_C decreases. However, in fact, little attention has been paid to the electromagnetic properties of $LaMnO_3$ oxides when only the Mn atoms on the B sites are partially replaced with other atoms.

It is well known that 3d magnetic metal ions form stable perovskite oxides together with rare-earth atoms which show various magnetic and transport behaviours. Mn^{3+} ions are ions

which induce Jahn–Teller distortion, and the ionic radius of Ni^{2+} is larger than that of Mn^{3+}. On the other hand, a theory of the role of covalence in the perovskite-type manganites was reported by Kanamori and Goodenough [12]. This theory indicates that the magnetic exchange interaction between Ni ions and Mn ions separated by an anion O^{2-} can be expected to be ferromagnetic. It would be interesting to study the charge mobility, CMR effect, and the Curie temperature from these points of view.

In this paper, Ni-doped La–Mn oxide samples are prepared and the electronic and magnetic properties are investigated. Another important requirement of this series is the random distribution of mixed-valence Mn ions. The Mn^{4+} ions can be produced either by deviation from the exact oxygen stoichiometry or by formation of vacancies or divalent-ion (divalent-hole) doping into the Mn sites of the parent $LaMnO_3$. The ratio of the concentrations Mn^{4+} and Mn^{3+} ions is also the ratio of Mn^{4+} to B sites, which is denoted by c. To analyse the dependence of T_C on the concentration of Ni (x) we apply the model of Varma [5, 14], which treats paramagnetic-to-FM (PM-to-FM) transition in La manganites by considering the electron localization due to magnetic disorder and the electron–electron interactions. We also discuss the dependence of the Mn^{4+} concentration on x by using Varma's model.

2. Experimental procedure

In order to investigate the CMR effect and magnetic properties of Ni-doped samples, we prepared samples with the compositions $LaMnO_3$ and $LaMn_{1-x}Ni_xO_3$ ($x = 0.01, 0.03, 0.1$) by the conventional solid-state reaction method. La_2O_3, MnO_2, and NiO powder were mixed in the appropriate ratio for more than 2 h, pressed into pellets, and calcined in air at 1223 K for 12 h. In the case of La_2O_3, in order to dehydrate $La(OH)_3$ completely into La_2O_3, the powder was heated in vacuum and then sealed in a glass tube. The appropriate ratio of MnO_2 and NiO was derived from the precise composition of the materials obtained by inductively coupled plasma (ICP) spectrometry. The pellets were ground for 2 h, pressed again, and sintered in air at 1473 K for 18 h.

The phases of prepared samples were identified by the x-ray powder diffraction method. Temperature dependence of magnetization (M–T curves) and magnetic field dependence (M–H curves) at several temperatures were measured by a vibrating-sample magnetometer (VSM). M–T curves were measured while applying a magnetic field of 0.1 T. The measurements were performed at temperature intervals of 20 K between 300 K and low temperature. The interval of the magnetic field was 0.5 T between +5 and −5 T. Resistivity was measured by the four-probe method, and the current direction was parallel to the magnetic field. The concentration of Mn^{4+} was determined by iodometric titrations using sodium thiosulphate.

3. Results and discussion

3.1. Structure and chemistry

The x-ray diffraction pattern of the $x = 0.01$ sample is shown in figure 1. The patterns of the other samples are similar to that of the $x = 0.01$ sample. All samples are perovskite single phase and the symmetry is rhombohedral. The influence of the Ni ratio on the structure is very small. In table 1, the ratio of Mn^{4+} ions (c) and the oxygen content measured by iodometric titrations together with the Curie temperature are shown. The results of ICP measurement indicate that the Mn concentration is in excess by several per cent, in contrast to the La concentration. It is found that the $x = 0.01$ sample has the highest Mn^{4+} concentration. This result is also obtained by replacement of Mn by Fe in our former results [13]. Though the valence of Mn in $LaMnO_3$ is basically Mn^{3+}, Mn^{4+} ions actually occupy 11% of B sites, which is probably due to the excess oxygen.

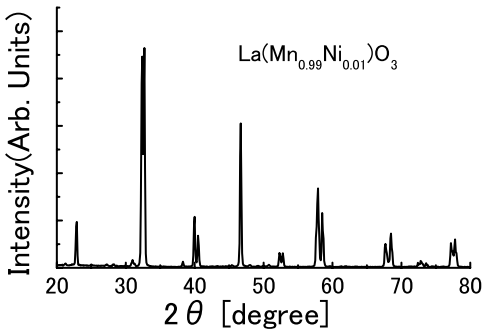

Figure 1. The x-ray diffraction pattern of the $x = 0.01$ sample.

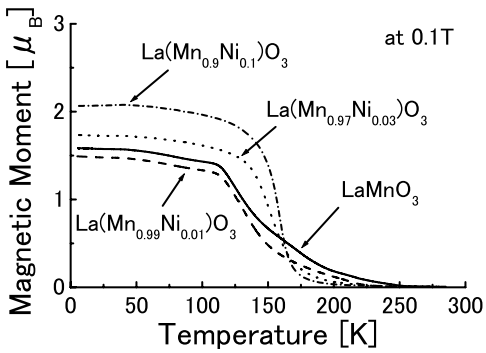

Figure 2. The temperature dependences of the magnetic moments of the samples. The applied magnetic field is 0.1 T.

Table 1. The Curie temperature, the concentration (c) of Mn^{4+}-occupied B sites, and the oxygen content of the samples.

x	T_C (K)	$c(x)$	Oxygen content
0	123	0.11	3.16
0.01	130	0.25	3.18
0.03	151	0.15	3.16
0.10	159	0.18	3.15

3.2. VSM measurements

The results on the temperature dependence of the magnetic moment measured by the VSM appear in figure 2. All samples are PM at room temperature and become FM on decreasing the temperature. The Curie temperatures, T_C, determined from the maximum point obtained from dM/dT, are also listed in table 1. There is a monotonic increase in T_C on increasing the Ni concentration. This tendency is opposite to the decrease in T_C with increasing Ni content seen in $La_{0.67}Sr_{0.33}Mn_{1-x}Ni_xO_3$ and $La_{0.67}Ca_{0.33}Mn_{1-x}Ni_xO_3$ [7, 20, 21].

Figure 2 shows that the magnetic moment of $LaMnO_3$ ($x = 0$) at low temperature is larger than that for $x = 0.01$, and smaller than those for $x = 0.03$ and 0.1. The effective Bohr magnetons of Mn^{3+}, Mn^{4+}, and Ni^{2+} ions are 4, 3, and 2, respectively. If the concentration of Mn^{3+}, which has the biggest effective Bohr magneton, decreases on doping with Ni, it can be

presumed that the magnetic moment should decrease. The smallest magnetic moment being shown by the $x = 0.01$ sample can be explained by the maximum content of Mn^{4+}, which has a smaller value of the effective Bohr magneton than Mn^{3+}. The results of iodometric titrations are qualitatively in good accordance with those from the M–T curves. But the magnetic moments of the $x = 0.03$ or 0.1 samples at low temperature become larger than that of $LaMnO_3$ on increasing the Mn^{4+} content, since the magnetic interactions between Ni^{2+} and Mn^{4+} or Mn^{3+} take on FM alignment, following Kanamori and Goodenough's rule [12].

3.3. The Mn^{4+} concentration

In the model of Varma, electrons are localized below the mobility threshold. Inside the band, the density of states has a rectangular shape with the bandwidth of W [5, 14]. According to this model, T_C satisfies the equation

$$k_B T_C \simeq 0.1 E^F_{coh}(c) \tag{1}$$

where $E^F_{coh}(c)$ is electronic cohesive energy in the FM phase:

$$E^F_{coh}(c) = \frac{Wc(1-c)}{2}. \tag{2}$$

To determine the relation between c and x, we take into account the possibility that cation vacancies which vary in concentration with x are generated during preparation of the samples. Here we assign $\delta(0)$ as the concentration of the vacancies in $LaMnO_3$ when no Mn ion is replaced by an Ni ion. Each vacancy of the B sites of $LaMn_{1-x}Ni_xO_{3+\alpha}$ yields three Mn^{4+} ions. An excess oxygen concentration α yields 2α Mn^{4+} ions. When Ni is doped into Mn sites, the Mn concentration apparently decreases. Assuming that the concentration of the vacancies in $LaMn_{1-x}Ni_xO_{3+\alpha}$, $\delta(x)$, becomes smaller than $\delta(0)$, the maximum possible decrease of the Mn concentration will be $x + \delta(0)$. We discuss how to distribute the Ni concentration, x, into the portions x and $\delta(0)$ in this $x + \delta(0)$ concentration. Taking into account that the probability, P, of the Ni concentration occupying the $\delta(0)$ portion is $P(x) = \delta(0)/(x + \delta(0))$, and that the actual Ni concentration in $\delta(0)$ will be xP, we obtain the Mn^{4+} concentration, $c(x) = x + 3\delta(x) + 2\alpha$, from electric neutrality as

$$c(x) = \frac{x^2 + (\delta(0) + 2\alpha)x + 3\delta(0)^2 + 2\delta(0)\alpha}{x + \delta(0)}. \tag{3}$$

Here, $\delta(x)$ is $\delta(0) - xP$, and the concentration of Mn is finally $1 - x - \delta(x)$. In order to consider the effect of the excess oxygen in detail, the relation between the Mn^{4+} concentration and x is derived for the following two models: (i) $\alpha \neq 0$ and (ii) $\alpha = 0$. Therefore, the fitting parameters of model (i) are W, δ, and α, while those of model (ii) are W and δ. Consequently, the relation between T_C and x can be derived from equations (1)–(3). The results of the curve fitting using equations (1)–(3) for the two models are shown in figures 3, 4 respectively.

Let us consider the relation equation between the Mn^{4+} concentration and x from a different angle, in order to consider Varma's equations (1), (2). Assuming that Mn and Ni evaporate during sintering in air at 1473 K, we can determine the Mn^{4+} concentration. We assign the defect concentrations of Mn and Ni as $\delta_{Mn}(x)$ and $\delta_{Ni}(x)$ respectively. Also the vapour pressures of Mn and Ni are assigned as P^0_{Mn} and P^0_{Ni}. We obtain the following equation:

$$\frac{\delta_{Ni}(x)}{\delta_{Mn}(x)} = \frac{P^0_{Ni}x}{P^0_{Mn}(1-x)}. \tag{4}$$

Using $c(x) = x - \delta_{Ni}(x) + 3\delta(x) + 2\alpha$, the Mn^{4+} concentration satisfies the equation

$$c(x) = x - \delta_{Ni}(x) + \frac{(0.178 + 0.822x)\delta_{Ni}(x)}{x} + 2\alpha. \tag{5}$$

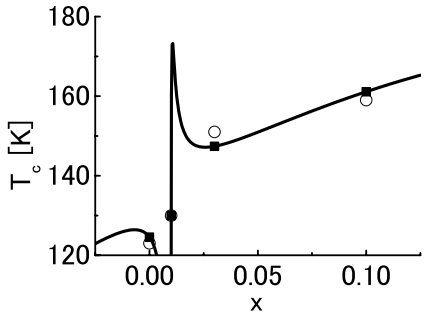

Figure 3. The dependence of T_C on x for the data from VSM (open spheres) and for models (i) (closed squares). The continuous curve resulted from the calculation over the whole x-range, using equations (1), (2), and model (i).

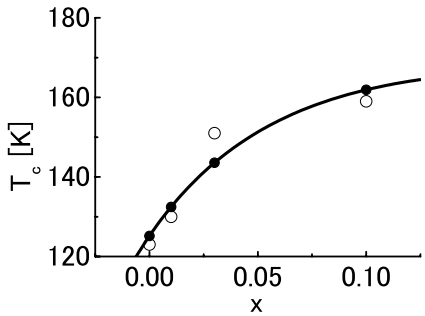

Figure 4. The dependence of T_C on x for the data from the VSM (open spheres) and for model (ii) (closed spheres). The continuous curve resulted from the calculation over the whole x-range, using equations (1), (2), and model (ii).

Table 2. The fitting parameters for models (i), (ii), and (iii).

	W (eV)	δ	α
Model (i)	1.20 ± 0.06	$-0.009\,44 \pm 0.000\,05$	0.131 ± 0.012
Model (ii)	1.23 ± 0.09	0.259 ± 0.010	Fixed
Model (iii)	1.10	$-0.006\,82$	0.20

What has to be noted is that $P^0_{Mn}/P^0_{Ni} = 0.178$ (the ratio of the vapour pressures at 1500 K [15]). As we can regard $\delta_{Ni}(x)$ as constant, the replacement concentration of Ni is less than $1/10$ of that of Mn, and also as P^0_{Ni} is about $1/5$ of that of Mn, P^0_{Mn}, at 1500 K, we can fit the dependence of T_C on x using equations (1), (2), and (5). We call this model (iii) (see figure 7). The fitting parameters of model (iii) are W, δ, and α.

Table 2 shows the fitted parameters for models (i), (ii), and (iii). Laiho *et al* [5] investigated the relation between T_C and x by using the same parameters as in our model (ii) for $La_{1-x}Ca_xMnO_3$ ($0 \leqslant x \leqslant 0.4$). They obtained that $W = 1.88 \pm 0.06$ eV and $\delta = 0.062 \pm 0.006$. Compared with their results, the W-values in our models (i), (ii), and (iii) are a little small. It is presumed that the excess Mn makes the values of δ in models (i) and (iii) negative. This is supported by the results on the (Mn + Ni)/La ratio obtained from ICP measurement, which are larger than 1 for our samples. Since δ of model (ii) is overestimated, model (ii) is incorrect for the samples which have excess oxygen.

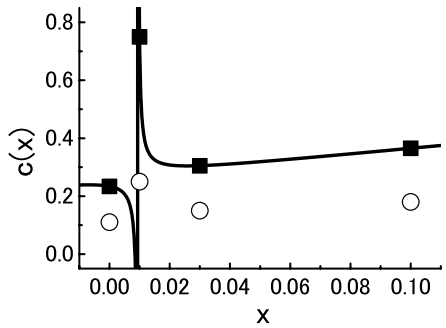

Figure 5. The dependence of $c(x)$ on x for model (i) (closed squares) and the content of Mn^{4+} obtained by iodometric titrations (open spheres).

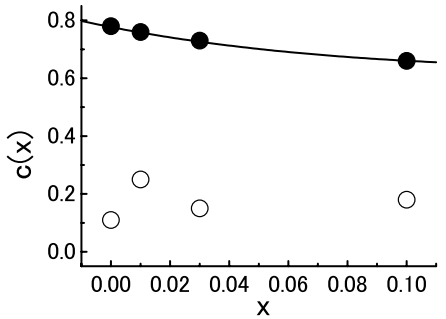

Figure 6. The dependence of $c(x)$ on x for model (ii) (closed spheres) and the content of Mn^{4+} obtained by iodometric titrations (open spheres).

Table 3. Composition (x) and the concentration of B sites occupied by Mn^{4+} (c) in the samples.

x	$c(x)$, model (i)	$c(x)$, model (ii)	$c(x)$, model (iii)	$c(x)$, iodometric titrations
0	0.23	0.78	—	0.11
0.01	0.75	0.76	0.29	0.25
0.03	0.31	0.73	0.39	0.15
0.1	0.37	0.66	0.49	0.18

The contents of Mn^{4+} ions obtained from the fit values of figures 3, 4, 7 are shown on figures 5, 6, 8, respectively. In table 3 the results of a survey of Mn^{4+} concentrations calculated from the figures 3, 4, 7 are also summarized. When compared with $c(x)$ obtained by iodometric titrations, that from model (i) is shown by table 2 to reproduce the increasing tendency of the Mn^{4+} concentration. Since $c(x)$ from model (iii) is not in good agreement with the tendency of increase in the Mn^{4+} concentration obtained by iodometric titrations, and also from examining figures 5, 6, 8, we see that the fitting curve of model (i) is the best. Quantitative agreement with iodometric titrations is not obtained, but the tendency of increase in Mn^{4+} concentration obtained by iodometric titrations is obtained by replacement of Mn with some Fe in our former results [13].

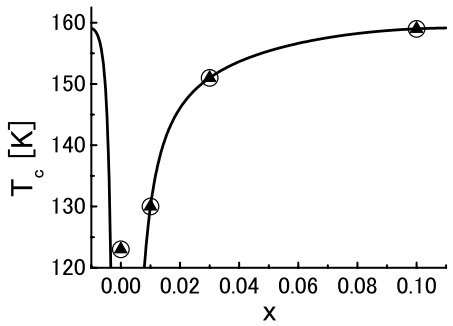

Figure 7. The dependence of T_C on x for the data from the VSM (open spheres) and for model (iii) (closed triangles). The continuous curve resulted from the calculation over the whole x-range, using equations (1), (2), and model (iii).

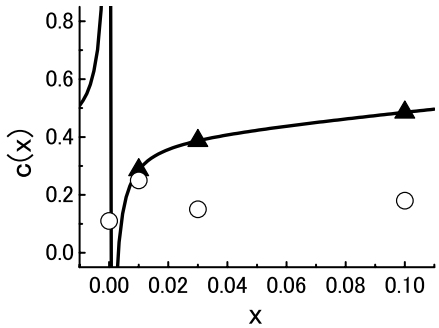

Figure 8. The dependence of $c(x)$ on x for model (iii) (closed triangles) and the content of Mn^{4+} obtained by iodometric titrations (open spheres).

3.4. Electronic resistivity

Figures 9 and 10 show the dependences of the resistivity and the magnitude of the CMR effect ($=(\rho_{0T}-\rho_{5\ T})/\rho_{0T}$ where ρ_{0T} and $\rho_{5\ T}$ are the resistivity when applying 0 and 5 T, respectively). The CMR effect is observed in all of the samples. Though the $LaMnO_{3+\alpha}$ sample exhibits a MIT, the other samples in which Ni is doped into Mn sites do not. Since our sample $LaMnO_{3+\alpha}$ has much excess oxygen, $\alpha = 0.16$, it is reasonable to suppose that many carriers are doped into the Mn–O–Mn network. Töpfer and Goodenough [16] reported that when $\alpha \geqslant 0.14$, a transition from localized itinerant charge carriers is observed below T_C. Therefore it is quite likely that the $LaMnO_{3+\alpha}$ sample shows a MIT. Some previous studies show that the structural, transport, and magnetic properties are affected by variations in oxygen content [16–19, 23]. The Mn^{4+} content increases when Ni is doped. However, the replacement of Mn with some Ni changes the sample to an insulator. We make the interpretation that Ni^{2+} disrupts the carrier mobility in the Mn–O–Mn network.

Ni-doped samples show CMR-effect maxima at temperatures near the Curie temperature, where the resistivity exponentially increases as temperature decreases. The $x = 0.01$ sample shows the largest CMR effect among all of the samples. One explanation for these experimental results is the high concentration of Mn^{4+} in the $x = 0.01$ sample. Since the $x = 0.01$ sample has the most excess oxygen among the samples, it has the highest Mn^{4+} content. It would be interesting to investigate the properties of samples which have exact stoichiometry with no excess oxygen in order to clarify the mechanism of the CMR effect quantitatively.

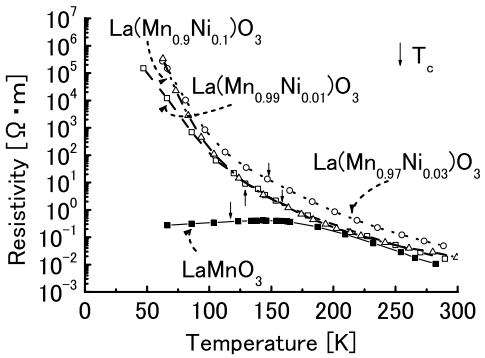

Figure 9. The temperature dependence of the resistivity.

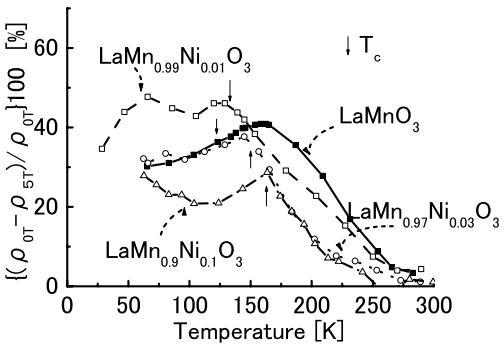

Figure 10. The temperature dependence of the CMR effect.

3.5. Magnetism and the CMR effect

It is concluded that the spin alignment of Mn^{3+} and Mn^{4+} in our samples is not antiferromagnetic, since $LaMnO_3$ is FM (figure 2), which is contrary to previous results. We presume that the excess oxygen and Ni at Mn sites cause the magnetic frustration and ferromagnetism in $LaMnO_{3+\alpha}$. A further extension of this study to $La(Mn, Ni)O_3$ would be necessary to examine the relation between the CMR effect, the excess oxygen, and the magnetic properties, such as spin glass and cluster glass properties [5, 16–19, 22–24]. In figure 11 the relation of the first maximum of the CMR effect and the magnetic moment at 0.1 T and 20 K is shown. The figure tells us that the CMR effect is small when Ni is doped into Mn sites. It can be seen that as the content Ni increases, samples become more FM. The $x = 0.01$ sample shows special behaviour here also.

4. Conclusions

The behaviour of the magnetic moment for $LaMn_{1-x}Ni_xO_{3+\alpha}$ ($x = 0, 0.01, 0.03, 0.10$) can be explained by the content of Mn^{4+}. The model, taking into account the excess oxygen using Varma's model, explains well the increasing tendency of the Mn^{4+} concentration when Ni is doped in. The samples are FM at low temperature. Though Ni-doped samples do not show MIT, they show a high CMR effect. The excess oxygen seems to be important to the CMR effect. This phenomena suggests that not only the double exchange but also some other mechanism is necessary to explain the origin of the CMR effect in this series of oxides.

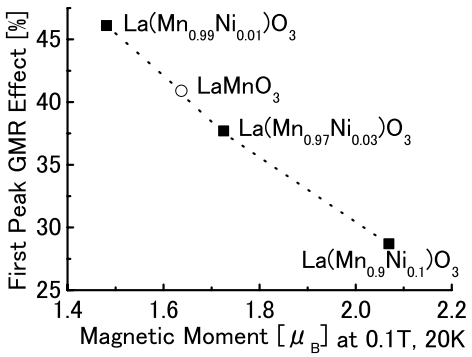

Figure 11. The magnetic moment at 0.1 T and 20 K and the maximum of the CMR effect.

Acknowledgments

The authors are grateful to Dr H Otsuka for the VSM measurements. This work was supported by a grant-in-aid for COE Research from the Ministry of Education, Science, Sports, and Culture (No 12CE2004 'Control of Electrons by Quantum Dot Structures and its Application to Advanced Electronics')

References

[1] Jonker G H and van Santen J H 1950 *Physica* **16** 337
[2] Jonker G H and van Santen J H 1953 *Physica* **19** 120
[3] Chahara K *et al* 1993 *Appl. Phys. Lett.* **63** 1990
[4] Hundley M F and Neumeier J J 1997 *Phys. Rev.* B **55** 11 511
[5] Laiho R *et al* 2000 *J. Phys.: Condens. Matter* **12** 5751
[6] Zener C 1951 *Phys. Rev.* **82** 403
[7] Wang Z H *et al* 2000 *J. Phys.: Condens. Matter* **12** 601
[8] Gayathri N *et al* 1997 *Phys. Rev.* B **56** 1345
[9] Ahn K H *et al* 1996 *Phys. Rev.* B **54** 15 299
[10] Raffaelle R *et al* 1991 *Phys. Rev.* B **43** 7991
[11] Medvedeva I V *et al* 2000 *Physica* B **292** 250
[12] Goodenough J B 1955 *Phys. Rev.* **100** 564
[13] Miwa Y 1999 *Master Thesis* University of Tokyo
[14] Varma C M 1996 *Phys. Rev.* B **54** 7328
[15] Barin I 1995 *Thermochemical Data for Pure Substances* vol T and U
[16] Töpfer J and Goodenough J B 1997 *Solid State Ion.* **101–3** 1215
[17] Zhao Y G *et al* 1999 *J. Appl. Phys.* **86** 6327
[18] Ritter C 1997 *Phys. Rev.* B **56** 8902
[19] Huang Q *et al* 1997 *Phys. Rev.* B **55** 14 987
[20] Wang Z H *et al* 1999 *J. Appl. Phys.* **85** 5399
[21] Rubinstein M *et al* 1997 *Phys. Rev.* B **56** 5412
[22] Krishnan R V and Banerjee A 2000 *J. Phys.: Condens. Matter* **12** 7887
[23] Kutty T R N and Philip J 2000 *J. Phys.: Condens. Matter* **12** 7747
[24] Itoh M *et al* 1994 *J. Phys. Soc. Japan* **63** 1486